RESEARCH ARTICLE

Editorial Process: Submission:06/04/2025 Acceptance:12/20/2025 Published:12/26/2025

Assessment of TrueBeam kV Cone-Beam CT Image Quality and the Clinical Impact of Calibration Drift

C O Clinto[1,2]*, B Bindhu[1]

Abstract

Background: This study compared the image quality of the TrueBeam (TB) kilo-voltage cone-beam CT (CBCT) system using standard reconstruction (TB-sCBCT) and iterative reconstruction (TB-iCBCT) with that of the Halcyon iterative CBCT (H-iCBCT). Additionally, the clinical impact of calibration drift over a one-year period was investigated for both head and pelvis imaging modes. **Methods:** Image quality and calibration were assessed using the Catphan®. Image quality evaluation included the analysis of signal-to-noise ratio (SNR), contrast-to-noise ratio (CNR), and low-contrast detectability. Calibration stability for head and pelvis CBCT modes was examined by comparing dose-volume histogram (DVH) parameters across ten tongue and ten prostate patient cases. **Results:** The average SNR was 3.1 for TB-sCBCT, 23.1 for TB-iCBCT, and 6.9 for H-iCBCT, while the corresponding CNR values were 11.2, 53.0, and 28.4, respectively. At a contrast level of 0.3%, the smallest detectable target diameters were 15 mm for TB-sCBCT, 8 mm for TB-iCBCT, and 9 mm for H-iCBCT. Over a one-year period, the Hounsfield Unit (HU) variation in the head CBCT mode exceeded the recommended action threshold of ±50 HU, whereas the pelvis CBCT mode remained within acceptable limits. **Conclusion:** In the TB system, advanced iterative reconstruction algorithms significantly enhance SNR and CNR by effectively reducing image noise. Halcyon provides improved image quality compared to TB with standard reconstruction; however, it remains inferior to TB-iCBCT. HU deviations were more pronounced in head CBCT than in pelvis mode, although HU variation in the pelvis CBCT mode exhibited greater sensitivity regarding clinical impact.

Keywords: CBCT image quality- iterative reconstruction- calibration drift

Asian Pac J Cancer Prev, **26 (12)**, 4563-4568

Introduction

Cone-beam computed tomography (CBCT) imaging systems have been integrated with medical linear accelerators for radiotherapy guidance [1, 2]. Compared to fan-beam CT (FBCT), cone-beam CT (CBCT) yields relatively lower image quality, primarily due to increased artifacts and scatter associated with its larger cone-beam geometry [3]. TrueBeam (TB) CBCT provides enhanced capabilities and improved imaging quality compared to the earlier On-Board Imaging CBCT systems of Varian Medical Systems [4]. The Feldkamp-Davis-Kress (FDK) algorithm, a variant of filtered back projection (FBP), remains the predominant reconstruction technique in CBCT due to its computational efficiency and simplicity, particularly for scans involving a large number of projections. However, advanced iterative reconstruction algorithms are increasingly being implemented to address limitations such as elevated image noise, reconstruction artifacts, and poor low-contrast resolution [5]. Varian Medical Systems developed the Halcyon platform as a streamlined and efficient solution for image-guided radiotherapy. In 2019, Jarema et al. [6] demonstrated the feasibility of utilizing Halcyon's iterative reconstruction cone-beam CT (iCBCT) images for radiation therapy planning in patients with pelvic cancers. Furthermore, Lassot-Buys et al. [7] showed that the iterative reconstruction algorithm implemented in Halcyon yields superior CBCT image quality compared to traditional filtered back projection techniques.

In 2006, Yoo et al. [8] evaluated the dosimetric feasibility of CBCT-based treatment planning, prompting extensive subsequent research in this area [9, 10]. As a result, CBCT, initially developed for image-guided radiotherapy (IGRT), has since been adopted for use in adaptive radiotherapy (ART) [11–16]. Accurate image calibration is essential for utilizing CBCT in radiation dose calculations, and several methods have been proposed for this purpose [17–20]. A widely accepted approach involves calibrating CBCT using phantoms with inserts of known mass density, electron density, or relative electron density (RED).

In 2009, Rong et al. [21] examined the stability of site-specific Hounsfield unit (HU)-to-density conversion by varying parameters such as mAs, source-to-imager distance, and cone angle at a tube voltage of 125 kV.

[1]Department of Physics, Noorul Islam Centre for Higher Education, Kumaracoil, Kanyakumari, Tamil Nadu, India. [2]Department of Radiation Oncology, Aster Medcity, Kochi, Kerala, India. *For Correspondence: clintoco@gmail.com

Their findings underscored the necessity of site-specific calibration to enhance the accuracy of CBCT-based dose calculations. Subsequent studies further investigated the stability of CBCT calibration and its dosimetric implications [22–24]. The EFOMP-ESTRO-IAEA quality control protocol by de Las et al. [25] recommends an action threshold of ±50 HU from baseline for dose calculation in radiation therapy. Schroder et al. [24] highlighted the need for scanner-specific calibration, while Souleyman et al. [26] demonstrated that selecting an appropriate CBCT acquisition protocol significantly influences dose calculation accuracy.

This study evaluated and compared the image quality of TrueBeam kilo-voltage CBCT acquired with standard reconstruction (TB-sCBCT) and iterative reconstruction (TB-iCBCT) to that of Halcyon iterative CBCT (H-iCBCT). Furthermore, the clinical implications of calibration drift over a one-year period were assessed for both head and pelvis imaging protocols.

Materials and Methods

Comparative analysis of image quality with the Halcyon system

In this study, CBCT images were acquired using the TrueBeam (version 3.0) and Halcyon (version 3.0) systems (Varian Medical Systems, Palo Alto, CA). The Catphan® 604 phantom (The Phantom Laboratory, USA) was used to evaluate image quality, as shown in Figure 1. The comparison of the TrueBeam and Halcyon kV-CBCT systems is shown in Table 1. Pelvis mode (125 kV, half-fan, full trajectory) was used for CBCT acquisition. Figure 2 shows the Catphan phantom setup used for image quality assessment on TrueBeam and Halcyon. Signal-to-noise ratio (SNR), contrast-to-noise ratio (CNR), and low-contrast visibility were assessed. SNR and CNR values were calculated using the following equations.

$$SNR = \frac{\mu}{\sigma} \quad \textbf{(Equation 1)}$$

$$CNR = \frac{P_{Object} - P_{Background}}{\sqrt{\sigma_O^2 + \sigma_B^2}} \quad \textbf{(Equation 2)}$$

Where, μ: mean pixel value; σ: standard deviation (noise); P: Pixel value.

Clinical impact of calibration drift

The clinical impact of calibration drift was assessed for both head and pelvis protocols of TB-sCBCT over a one-year period. The exposure parameters were set as standard imaging protocols for the Head (100 kVp, 270 mAs, full fan) and Pelvis (125 kVp, 1074 mAs, half fan). The CTP404 module of the Catphan® 504 (The Phantom Laboratory, USA) was used for calibrating CBCT image. The initial HU-RED table was used as the baseline and compared with the subsequent calibration curves. Volumetric modulated arc therapy (VMAT) plans on CBCT images for ten tongue and ten prostate cancer patients were evaluated. The HU-RED curves measured after 6 months, 1 year, and post-calibration were updated in the same plan and recalculated using the anisotropic analytical algorithm (Version 13.7.16). For the tongue cases, the dose received by 95% of the planning target volume (D95%) and the maximum doses to the spinal cord and brainstem were compared. For the prostate cases, the dose received by 95% of the planning target volume (D95) and the volume receiving 45Gy (V45Gy) to the bladder and rectum were compared.

Statistical Analysis

Statistical analyses were performed using SPSS software (version 21.0; SPSS Inc., Chicago, IL, USA). Comparisons of dose-volume histogram (DVH) parameters across different time points were conducted using repeated measures ANOVA, followed by the least significant difference (LSD) test to identify statistically significant differences. Superscripts in the tables indicate statistical groupings. Identical superscripts denote no significant difference between groups, whereas different superscripts (e.g., a, b, c) signify that the corresponding means differ significantly based on the LSD test. A P-value of less than 0.01 was considered statistically significant.

Results

Image quality: TrueBeam Vs Halcyon

The SNR values at different regions of uniformity module for TrueBeam and Halcyon is shown in Table 2.

Table 1. Comparison of kV-CBCT Systems in TrueBeam (version 3.0) and Halcyon (version 3.0)

Parameter	TrueBeam 3.0	Halcyon 3.0
Detector Type	Amorphous silicon with Cesium Iodide scintillator	Amorphous silicon with Gadolinium Oxysulfide scintillator
Source to Imager Distance	150 cm	154 cm
Isocenter to Detector Distance	50 cm	54 cm
Maximum Gantry Speed	1 RPM	4 RPM
Full Scan Time	~ 60 Sec	15-17 Sec

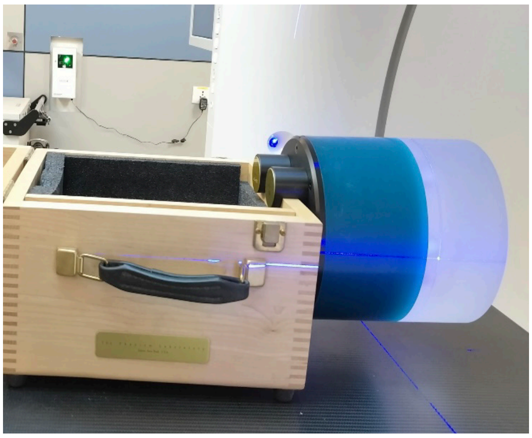

Figure 1. Catphan® 604 phantom

Table 2. SNR (Signal-to-Noise Ratio) at Different Regions of Uniformity Module of the Catphan®

	TrueBeam CBCT						Halcyon		
	sCBCT			iCBCT			kV CBCT		
ROI	Mean Pixel	SD	SNR	Mean Pixel	SD	SNR	Mean Pixel	SD	SNR
Centre	6.8	2.0	3.5	-13.3	0.6	22.2	11.4	1.8	6.3
Right	5.2	1.5	3.4	-16.8	0.7	25.1	13.6	2.0	7.0
Left	5.0	2.1	2.4	-16.0	1.4	11.2	11.1	2.4	4.7
Top	4.6	1.5	3.0	-15.2	0.6	23.7	18.5	2.0	9.1
Bottom	4.4	1.3	3.4	-15.0	0.5	33.4	11.3	1.5	7.5

Figure 2. Catphan® Phantom Setup for Image Quality Assessment on (A) TrueBeam and (B) Halcyon.

Table 3. Contrast-to-Noise Ratio (CNR) of CBCT Images Estimated Using Catphan®

	TrueBeam sCBCT			TrueBeam iCBCT			Halcyon kV-CBCT		
	Mean Pixel	SD	CNR	Mean Pixel	SD	CNR	Mean Pixel	SD	CNR
Acrylic	116.1	3.2	11.2	96.3	1.1	53.0	126.3	2.0	28.4
Background	50.6	4.9		29.9	0.6		53.2	1.7	

Table 4. Smallest Object Discernible for Different Contrast Levels in CBCT Images

Contrast level	Smallest diameter discernible (mm)		
	TrueBeam sCBCT	TrueBeam iCBCT	Halcyon kV-CBCT
1%	4	3	4
0.50%	9	8	8
0.30%	15	8	9

Table 3 shows the CNR comparison between TrueBeam and Halcyon. The low-contrast visibility comparison presented in Table 4.

Clinical impact of calibration drift

Figures 3 and 4 show the changes in calibration curves over the course of one year and after HU calibration for the head and pelvis CBCT protocols, respectively. The HU variability was more pronounced for the head

Table 5. HU Differences Over the Course of One Year and Following Imager CAL

RED	HU Difference					
	CBCT Head Protocol			CBCT Pelvis Protocol		
	After 6M	After 1Y	After CAL	After 6M	After 1Y	After CAL
0	0	-1	1	-2	-2	0
0.853	-15	0	2	1	-9	-1
0.944	-4	11	4	5	-7	0
1.017	-8	8	-8	2	-7	-3
1.146	10	30	-8	-3	-18	3
1.354	24	40	-14	-10	-25	0
1.867	40	80	-17	-7	-26	0

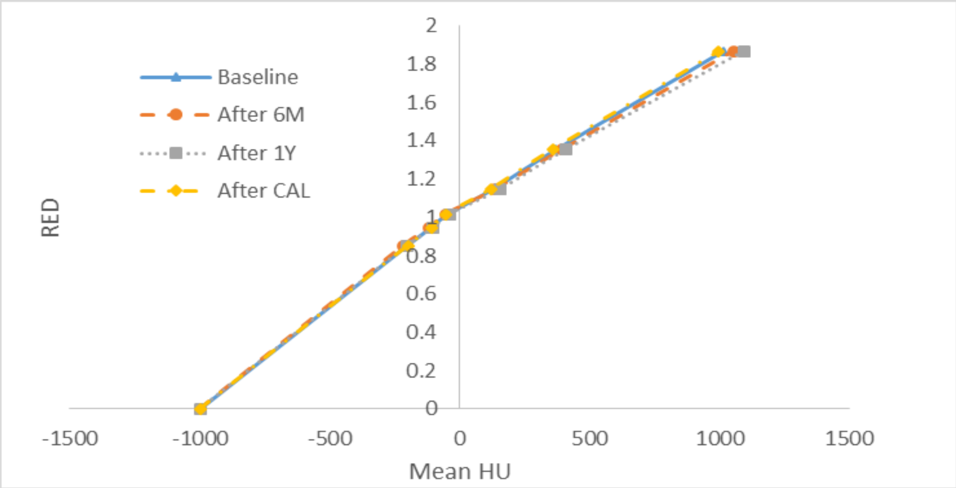

Figure 3. Calibration Curves for the CBCT Head Protocol after 6 Months, 1 Year, and Following Imager Calibration (CAL)

Table 6. DVH Parameters of Tongue Cancer Patients with Change in HU-RED Curve

DVH Parameter	Mean percentage deviation (%)			
	After 6M	After 1Y	After CAL	P-value
PTV 66: D95%	0.037[b]	0.288[a]	0.007[b]	<0.001
PTV 60: D95%	0.036[b]	0.292[a]	-0.021[c]	<0.001
Spinal cord: Dmax	-0.003[b]	0.200[a]	-0.010[b]	<0.001
Brainstem: Dmax	0.154[b]	0.501[a]	-0.093[c]	<0.001

*Different superscripts (a, b, c) denote significant differences between means

protocol compared to the pelvis, as shown in Table 5. Table 6 presents the deviations in DVH parameters for tongue cancer patients in relation to changes in the HU-RED curve. Over the period of one year, 0.3% deviation observed in targets coverage and 0.2% and 0.5% deviations in maximum dose to spinal cord and brainstem respectively. Table 7 presents the deviations in DVH parameters for prostate patients associated with changes

Table 7. DVH Parameters of Prostate Cancer Patients with Change in HU-RED Curve

DVH Parameter	Mean percentage deviation (%)			
	After 6M	After 1Y	After CAL	P-value
PTV: D95%	0.028[a]	-0.471[c]	-0.012[b]	<0.001
Bladder: V45Gy	0.122[a]	-0.413[c]	0.001[b]	<0.001
Rectum: V45Gy	0.044[a]	-0.442[c]	-0.012[b]	<0.001

*Different superscripts (a, b, c) denote significant differences between means.

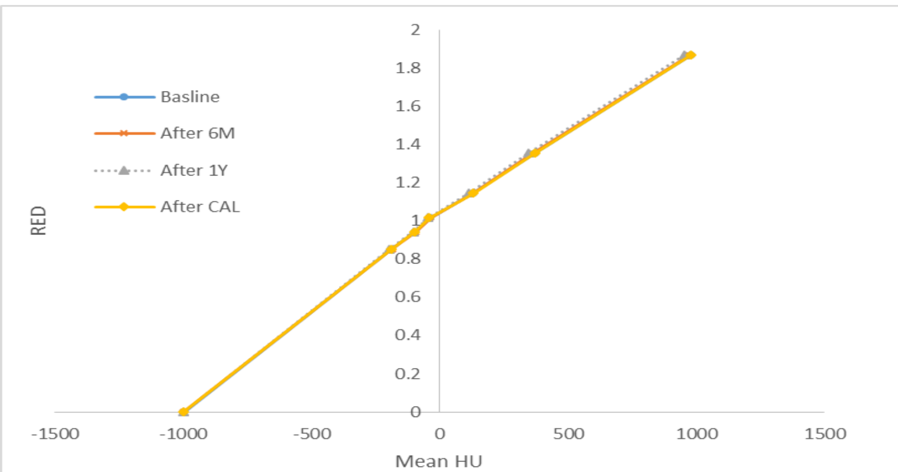

Figure 4. Calibration Curves for the CBCT Pelvis Protocol after 6 Months, 1 Year, and Following Imager CAL

in the HU-RED curve. The D95% of the PTV showed a deviation of -0.5%, while the V45Gy deviations were -0.4% for both the bladder and rectum. The HU calibration of the CBCT system substantially reduced the deviation for both cases.

Discussion

High image quality and stable calibration are crucial for ensuring accurate dose calculations when using CBCT images in adaptive radiotherapy. Gardner et al. [5] reported enhancements in image uniformity, noise reduction, and overall image quality with iterative CBCT reconstruction. Similarly, Lim et al. [27] demonstrated statistically significant improvements in image quality using the Catphan phantom when comparing iterative CBCT to conventional FDK-based CBCT. Washio et al. [28] noted an enhancement in low-contrast detectability through iterative reconstruction, along with a reduction in patient dose. Both TrueBeam and Halcyon systems utilize iterative reconstruction algorithms to improve image quality [29]. Their performance varies due to hardware design and acquisition differences. TrueBeam, with a larger flat-panel detector (Varian PaxScan 4030CB) and a 150 cm source-to-imager distance, provides a wider field-of-view (FOV) and higher resolution. Halcyon, equipped with a smaller detector (PaxScan 4030DX) and a 154 cm distance, offers a slightly narrower FOV. While TrueBeam requires longer scan times, it delivers superior HU accuracy, image uniformity, and lower noise. Halcyon enables faster scans but at the cost of slightly higher noise and reduced soft-tissue contrast due to limited photon statistics. While TrueBeam iCBCT demonstrates superior performance, particularly in SNR, CNR, and low-contrast detectability, Halcyon iCBCTthough designed for clinical efficiency shows slightly lower image quality in comparison.

The differences observed in calibration curves across CBCT modes suggest that using parameter-specific calibration curves could improve dosimetric accuracy, as recommended by Souleyman et al. [26]. The HU variation was more prominent in head CBCT than in pelvis mode, exceeding the EFOMP-ESTRO-IAEA recommended action threshold of ±50 HU over the course of one year.

Since CBCT numbers (HU) are influenced by multiple parameters, they vary considerably with changes in x-ray energy. The head protocol, which employs lower energy (100 kVp), results in increased scatter and consequently greater HU variability due to image noise

Over the course of one year, the clinical impact was within ±0.5%. Since HU-RED calibration is a controllable parameter, reducing its drift can enhance treatment outcomes. This underscores the importance of scanner- and protocol-specific calibration at more frequent testing intervals as reported by Schroder et al [24]. The clinical impact of calibration drift may differ depending on the clinical context, such as the target area's location, adjacent critical structures, and the specific treatment protocol used. Adaptive plans are created using CBCT images to produce adapted PTVs and planning organ-at-risk (OAR) volumes [30-32]. The image quality and frequent calibration can help to reduce the uncertainties in CBCT-based treatment planning.

In TrueBeam, advanced iterative reconstruction algorithms improve SNR and CNR by effectively reducing noise while maintaining contrast. Halcyon offers better image quality compared to TrueBeam with standard reconstruction but falls short when compared to TrueBeam iCBCT. The HU difference was more noticeable in head CBCT compared to pelvis mode; however, HU variation in pelvis CBCT mode showed greater dosimetric sensitivity. The clinical impact due to the calibration drift over the course of one year was within ±0.5%.

Author Contribution Statement

Both authors contributed equally to this study.

Acknowledgements

We are thankful to Regional Cancer Centre, Thiruvanathapuram and Caritas Hospital, Kottayam for providing facility for image quality comparison. This study forms part of the Ph.D. program registered at Noorul Islam Center for Higher Education, Kanyakumari, and has been approved by the Doctoral Committee.

Conflicts of Interest

There are no conflicts of interest in this study.

References

1. Oelfke U, Tücking T, Nill S, Seeber A, Hesse B, Huber P, et al. Linac-integrated kv-cone beam ct: Technical features and first applications. Med Dosim. 2006;31(1):62-70. https://doi.org/10.1016/j.meddos.2005.12.008.
2. Saw CB, Yang Y, Li F, Yue NJ, Ding C, Komanduri K, et al. Performance characteristics and quality assurance aspects of kilovoltage cone-beam ct on medical linear accelerator. Med Dosim. 2007;32(2):80-5. https://doi.org/10.1016/j.meddos.2007.01.003.
3. Lechuga L, Weidlich GA. Cone beam ct vs. Fan beam ct: A comparison of image quality and dose delivered between two differing ct imaging modalities. Cureus. 2016;8(9):e778. https://doi.org/10.7759/cureus.778.
4. Kawahara D, Ozawa S, Nakashima T, Suzuki T, Tsuneda M, Tanaka S, et al. Absorbed dose and image quality of varian truebeam cbct compared with obi cbct. Phys Med. 2016;32(12):1628-33. https://doi.org/10.1016/j.ejmp.2016.11.118.
5. Gardner SJ, Mao W, Liu C, Aref I, Elshaikh M, Lee JK, et al. Improvements in cbct image quality using a novel iterative reconstruction algorithm: A clinical evaluation. Adv Radiat Oncol. 2019;4(2):390-400. https://doi.org/10.1016/j.adro.2018.12.003.
6. Jarema T, Aland T. Using the iterative kv cbct reconstruction on the varian halcyon linear accelerator for radiation therapy planning for pelvis patients. Phys Med. 2019;68:112-6. https://doi.org/10.1016/j.ejmp.2019.11.015.
7. Lassot-Buys M, Verstraet R, Dabli D, Moliner G, Greffier J. Task-based image quality assessment comparing classical and iterative cone beam ct images on halcyon(®). Diagnostics (Basel). 2023;13(3):448. https://doi.org/10.3390/diagnostics13030448.
8. Yoo S, Yin FF. Dosimetric feasibility of cone-beam ct-based

treatment planning compared to ct-based treatment planning. Int J Radiat Oncol Biol Phys. 2006;66(5):1553-61. https://doi.org/10.1016/j.ijrobp.2006.08.031.
9. Yang Y, Schreibmann E, Li T, Wang C, Xing L. Evaluation of on-board kv cone beam ct (cbct)-based dose calculation. Phys Med Biol. 2007;52(3):685-705. https://doi.org/10.1088/0031-9155/52/3/011.
10. de Smet M, Schuring D, Nijsten S, Verhaegen F. Accuracy of dose calculations on kv cone beam ct images of lung cancer patients. Med Phys. 2016;43(11):5934. https://doi.org/10.1118/1.4964455.
11. Jassim H, Nedaei HA, Geraily G, Banaee N, Kazemian A. The geometric and dosimetric accuracy of kilovoltage cone beam computed tomography images for adaptive treatment: A systematic review. BJR Open. 2023;5(1):20220062. https://doi.org/10.1259/bjro.20220062.
12. Hansen EK, Bucci MK, Quivey JM, Weinberg V, Xia P. Repeat ct imaging and replanning during the course of imrt for head-and-neck cancer. Int J Radiat Oncol Biol Phys. 2006;64(2):355-62. https://doi.org/10.1016/j.ijrobp.2005.07.957.
13. Schwartz DL, Dong L. Adaptive radiation therapy for head and neck cancer-can an old goal evolve into a new standard? J Oncol. 2011;2011. https://doi.org/10.1155/2011/690595.
14. Branco D, Mayadev J, Moore K, Ray X. Dosimetric and feasibility evaluation of a cbct-based daily adaptive radiotherapy protocol for locally advanced cervical cancer. J Appl Clin Med Phys. 2023;24(1):e13783. https://doi.org/10.1002/acm2.13783.
15. de Jong R, Visser J, van Wieringen N, Wiersma J, Geijsen D, Bel A. Feasibility of conebeam ct-based online adaptive radiotherapy for neoadjuvant treatment of rectal cancer. Radiat Oncol. 2021;16(1):136. https://doi.org/10.1186/s13014-021-01866-7.
16. van de Schoot AJ, Hoffmans D, van Ingen KM, Simons MJ, Wiersma J. Characterization of ethos therapy systems for adaptive radiation therapy: A multi-machine comparison. J Appl Clin Med Phys. 2023;24(5):e13905. https://doi.org/10.1002/acm2.13905.
17. Hatton J, McCurdy B, Greer PB. Cone beam computerized tomography: The effect of calibration of the hounsfield unit number to electron density on dose calculation accuracy for adaptive radiation therapy. Phys Med Biol. 2009;54(15):N329-46. https://doi.org/10.1088/0031-9155/54/15/n01.
18. Dunlop A, McQuaid D, Nill S, Murray J, Poludniowski G, Hansen VN, et al. Comparison of ct number calibration techniques for cbct-based dose calculation. Strahlenther Onkol. 2015;191(12):970-8. https://doi.org/10.1007/s00066-015-0890-7.
19. Giacometti V, King RB, Agnew CE, Irvine DM, Jain S, Hounsell AR, et al. An evaluation of techniques for dose calculation on cone beam computed tomography. Br J Radiol. 2019;92(1096):20180383. https://doi.org/10.1259/bjr.20180383.
20. Giacometti V, Hounsell AR, McGarry CK. A review of dose calculation approaches with cone beam ct in photon and proton therapy. Phys Med. 2020;76:243-76. https://doi.org/10.1016/j.ejmp.2020.06.017.
21. Rong Y, Smilowitz J, Tewatia D, Tomé WA, Paliwal B. Dose calculation on kv cone beam ct images: An investigation of the hu-density conversion stability and dose accuracy using the site-specific calibration. Med Dosim. 2010;35(3):195-207. https://doi.org/10.1016/j.meddos.2009.06.001.
22. Yadav P, Ramasubramanian V, Paliwal BR. Feasibility study on effect and stability of adaptive radiotherapy on kilovoltage cone beam ct. Radiol Oncol. 2011;45(3):220-6. https://doi.org/10.2478/v10019-011-0024-5.
23. Takemura A, Tanabe S, Tokai M, Ueda S, Noto K, Isomura N, et al. Long-term stability of the hounsfield unit to electron density calibration curve in cone-beam computed tomography images for adaptive radiotherapy treatment planning. J Radiother Pract. 2015;14(4):410-7. https://doi.org/10.1017/S1460396915000321.
24. Schröder L, Stankovic U, Sonke JJ. Technical note: Long-term stability of hounsfield unit calibration for cone beam computed tomography. Med Phys. 2020;47(4):1640-4. https://doi.org/10.1002/mp.14015.
25. de Las Heras Gala H, Torresin A, Dasu A, Rampado O, Delis H, Hernández Girón I, et al. Quality control in cone-beam computed tomography (cbct) efomp-estro-iaea protocol (summary report). Phys Med. 2017;39:67-72. https://doi.org/10.1016/j.ejmp.2017.05.069.
26. Souleyman S, Maria KD, Cheikh T, Karima KK. Impact of acquisition protocols on accuracy of dose calculation based on xvi cone beam computed tomography. J Med Phys. 2021;46(2):94-104. https://doi.org/10.4103/jmp.JMP_128_20.
27. Lim R, Penoncello GP, Hobbis D, Harrington DP, Rong Y. Technical note: Characterization of novel iterative reconstructed cone beam ct images for dose tracking and adaptive radiotherapy on l-shape linacs. Med Phys. 2022;49(12):7715-32. https://doi.org/10.1002/mp.15943.
28. Washio H, Ohira S, Funama Y, Ueda Y, Morimoto M, Kanayama N, et al. Dose reduction and low-contrast detectability using iterative cbct reconstruction algorithm for radiotherapy. Technol Cancer Res Treat. 2022;21:15330338211067312. https://doi.org/10.1177/15330338211067312.
29. Varian Medical Systems. Varian's Iterative Cone-Beam Computed Tomography (iCBCT): Clear Soft Tissue Visualization for Precision Radiotherapy [Internet]. [Updated 2020 Feb 24]. Available from: https://www.varian.com/varians-iterative-cone-beam-computed-tomography-icbct-clear.
30. Meyers SM, Winter JD, Obeidi Y, Chung P, Menard C, Warde P, et al. A feasibility study of adaptive radiation therapy for postprostatectomy prostate cancer. Med Dosim. 2024;49(2):150-8. https://doi.org/10.1016/j.meddos.2023.10.008.
31. Moallim M, Maungwe P, Chamunyonga C. Cbct-guided radiotherapy for locally advanced head and cancer: Dosimetric impact of weight loss on vmat and imrt plans for selected organs at risk structures (oars). J Radiother Pract. 2015;14(4):336-42. https://doi.org/10.1017/S1460396915000291.
32. Srivastava D, Sharma PK, Maria Das KJ, Jayanand D. A hybrid approach for head and neck cancer using online image guidance and offline adaptive radiotherapy planning. J Radiother Pract. 2019;18(3):271-5. https://doi.org/10.1017/S146039691800078X.

This work is licensed under a Creative Commons Attribution-Non Commercial 4.0 International License.